



## 저작자표시 2.0 대한민국

이용자는 아래의 조건을 따르는 경우에 한하여 자유롭게

- 이 저작물을 복제, 배포, 전송, 전시, 공연 및 방송할 수 있습니다.
- 이차적 저작물을 작성할 수 있습니다.
- 이 저작물을 영리 목적으로 이용할 수 있습니다.

다음과 같은 조건을 따라야 합니다:



저작자표시. 귀하는 원저작자를 표시하여야 합니다.

- 귀하는, 이 저작물의 재이용이나 배포의 경우, 이 저작물에 적용된 이용허락조건을 명확하게 나타내어야 합니다.
- 저작권자로부터 별도의 허가를 받으면 이러한 조건들은 적용되지 않습니다.

저작권법에 따른 이용자의 권리는 위의 내용에 의하여 영향을 받지 않습니다.

이것은 [이용허락규약\(Legal Code\)](#)을 이해하기 쉽게 요약한 것입니다.

[Disclaimer](#) 

M.S. THESIS

# Gas Sensing Characterization of Single Layer Graphene Prepared by ICP-CVD Method

ICP-CVD방법에 의해 형성된  
단층 그래핀의 가스 반응 특성

BY

CHANGHEE KIM

August 2012

DEPARTMENT OF ELECTRICAL ENGINEERING AND  
COMPUTER SCIENCE  
COLLEGE OF ENGINEERING  
SEOUL NATIONAL UNIVERSITY

# Gas Sensing Characterization of Single Layer Graphene Prepared by ICP-CVD Method

ICP-CVD방법에 의해 형성된  
단층 그래핀의 가스 반응 특성

지도교수 이종호

이 논문을 공학석사 학위논문으로 제출함

2012년 8월

서울대학교 대학원

전기컴퓨터공학부

김 창 희

김창희의 공학석사 학위논문을 인준함

2012년 8월

위원장 : 박 병 국 (인)

부위원장 : 이 종 호 (인)

위원 : 홍 용 택 (인)

# ABSTRACT

Recently, there has been an increased demand for low cost, highly sensitive and selective gas sensing devices. Graphene, single atomic layer of graphite, has been considered as very attractive as gas sensor device application (The graphene have higher sensitivities for NO<sub>2</sub> and NH<sub>3</sub>). In the past few years, there have been mechanical exfoliation method using scotch tape and many chemical approaches to synthesize large-scale graphene have been developed, including epitaxial growth on silicon carbide at high temperature (1450 °C), formation of graphene in ultra-high vacuum environment and chemical vapor deposition (CVD). Recently it becomes increasingly important to form high-quality graphene layer at lower process temperature to be applied to flexible electronics. As a good candidate, Inductively-Coupled Plasma Chemical Vapor Deposition (ICP-CVD) was used to form graphene at 650 °C. However, there have been no reports on gas sensitivity and temperature effect of graphene FET by ICP-CVD method.

In this master's thesis, we report gas sensitivity and effect of temperature ( $T$ ) and relative humidity (RH) on gas sensitivity of the bottom-gate graphene FETs with single atomic layer of channel graphene fabricated by ICP-CVD method. The graphene FETs have relatively higher sensitivities for  $\text{NH}_3$  (~20% at 50 ppm) and  $\text{NO}_2$  (~30% at 50 ppm). Other gases such as  $\text{CH}_4$ ,  $\text{C}_3\text{H}_8$ ,  $\text{H}_2\text{S}$ , and  $\text{SO}_2$  show a sensitivity of less than ~10% at even  $10^4$  ppm. The sensitivity of graphene exposed to nitrogen oxide ( $\text{NO}_2$ ) and ammonia ( $\text{NH}_3$ ) was increased with increasing temperature and humidity. For  $\text{NO}_2$  gas, the graphene FET shows increasing  $I_D$  with increasing  $T$  and also increasing  $I_D$  with increasing humidity. However, the FET shows opposite trend with the  $T$  and humidity for  $\text{NH}_3$  gas. We observed that gases produce distinguishably different effects on the low-frequency noise spectra of graphene. These characterizations could be used to design more reliable graphene gas sensor.

**Keywords:** graphene, gas sensor, selectivity, bottom gate FET, inductively coupled plasma chemical vapor deposition (ICP-CVD), temperature, humidity, low frequency noise.

Student number: 2010-23254

# CONTENTS

<b>Abstract</b>	-----	<b>i</b>
<b>Contents</b>	-----	<b>iii</b>
<b>1. Introduction</b>	-----	<b>1</b>
<b>2. Fabrication Process and Surface Characterization</b>	-----	<b>4</b>
<b>2.1 Fabrication Process</b>	-----	<b>4</b>
<b>2.2 Surface characterization</b>	-----	<b>7</b>
<b>3. Analysis of Gas sensing Characterization on Bottom Gate</b>		
<b>Graphene FET</b>	-----	<b>10</b>
<b>3.1 Gas Sensing on bottom gate graphene FET</b>	-----	<b>10</b>

<b>3. 2 Effect of Temperature and Humidity on NO<sub>2</sub> and NH<sub>3</sub> Gas Sensitivity of Bottom-Gate Graphene FETs</b>	<b>17</b>
<b>4. Conclusion</b>	<b>24</b>
<b>References</b>	<b>25</b>
<b>Abstract in Korean</b>	<b>30</b>

# 1. Introduction

Zero band gap graphene (a single atomic layer of graphite sheet) have awakened an enormous interest in this two- dimensional material. Owing to its unique structural, mechanical and electronic properties, graphene is considered as most attractive candidates for next generation electronic device application, ranging from chemical sensor, DNA sequencing, and transparent electrodes [1]. In the past few years, there have been mechanical exfoliation method using scotch tape [2] and many chemical approaches to synthesize large-scale graphene have been developed, including epitaxial growth on silicon carbide at high temperature (1450 °C), formation of graphene in ultra-high vacuum environment and chemical vapor deposition (CVD) [3]. Recently, there has been an increased interest in highly sensitive and selective gas sensing devices to detect air contaminants released from industrial complexes and automobiles because they have caused smog and lung diseases such as asthma [4]. As one of

sensing materials for future gas sensors, single-layer graphene has been applied to the channel material in FET type gas sensor which detects the conductivity change upon adsorption of gases ( $\text{NO}_2$ ,  $\text{NH}_3$ ) [1]. In [1], the graphene was prepared by a mechanical exfoliation method and authors reported only the sensitivity. The sensitivity was studied with temperature in graphene FET where the graphene was implemented by a mechanical exfoliation [5], epitaxial growth on silicon carbide at high temperature [6] and CVD method [7]. Recently it becomes increasingly important to form high-quality graphene layer at lower process temperature to be applied to flexible electronics. As a good candidate, ICP-CVD was used to form graphene at 650 °C. There have been no reports on sensitivity and temperature effect of graphene FET by ICP-CVD method. Moreover, the gas sensitivity and the sensing property on humidity have not been reported in detail.

In chapter 2, the fabrication process and surface characterization of graphene are introduced. The Raman spectroscopy and optical transmittance spectroscopy were used for characterizing the single layer graphene.

In chapter 3, we quantitatively analyzed the gas sensing characterization of graphene such gas sensitivity, effect of temperature and humidity on NO<sub>2</sub> and NH<sub>3</sub> gas sensitivity. The mechanism of gas sensing on graphene are researched.

## **2. Fabrication Process and Surface characterization**

### **2.1 Fabrication Process**

Key fabrication process steps and resultant device structure are shown in Fig.

1.  $\text{HfO}_2$  (30 nm) is deposited by Atomic Layer Deposition (ALD) method as gate dielectric on the heavily doped 6-inch N-type silicon wafer which is used as bottom-gate electrode. Then, source and drain electrodes are formed by electron-beam evaporation of Cr/Au. Finally, the oxygen plasma etching was adapted for the definition of graphene channel. The graphene layer was formed by using plasma assisted CVD at a low temperature of 650 °C. More detailed explanation on the process can be found in [8]. Graphene in this study are synthesized by inductively coupled plasma enhanced chemical vapor deposition (ICP-CVD) on a Cu thin film substrate. During the growth process, the substrate is heated to

650°C within 10 min under  $\sim 10^{-7}$  torr, then treated with H<sub>2</sub> plasma. After purging with Ar for a couple of minutes, C<sub>2</sub>H<sub>2</sub> is added (C<sub>2</sub>H<sub>2</sub>: Ar = 1: 40) for graphene growth at the same temperature. For the graphene transfer, graphene/metal/SiO<sub>2</sub>/Si substrate was spin-coated with PMMA (Aldrich, 950 A4) and attached a pressure sensitive adhesive ultraviolet tape. Peeling the tape against the Si wafer physically separates the tape/PMMA/graphene/metal layer due to poor adhesion of the metal film and SiO<sub>2</sub>. After etching of the underlying Ni/Cu by soaking in FeCl<sub>3</sub> and cleaning in water, the tape/PMMA/graphene layer was pressed onto the HfO<sub>x</sub> (30 nm)/Si substrate with pre-patterned electrodes (Cr/Au of 10/90 nm). The successive removal of the tape and PMMA in methanol and acetone, respectively, leaves only the graphene layer over the pre-patterned marks. Graphene is etched to rectangular shape by O<sub>2</sub> plasma.

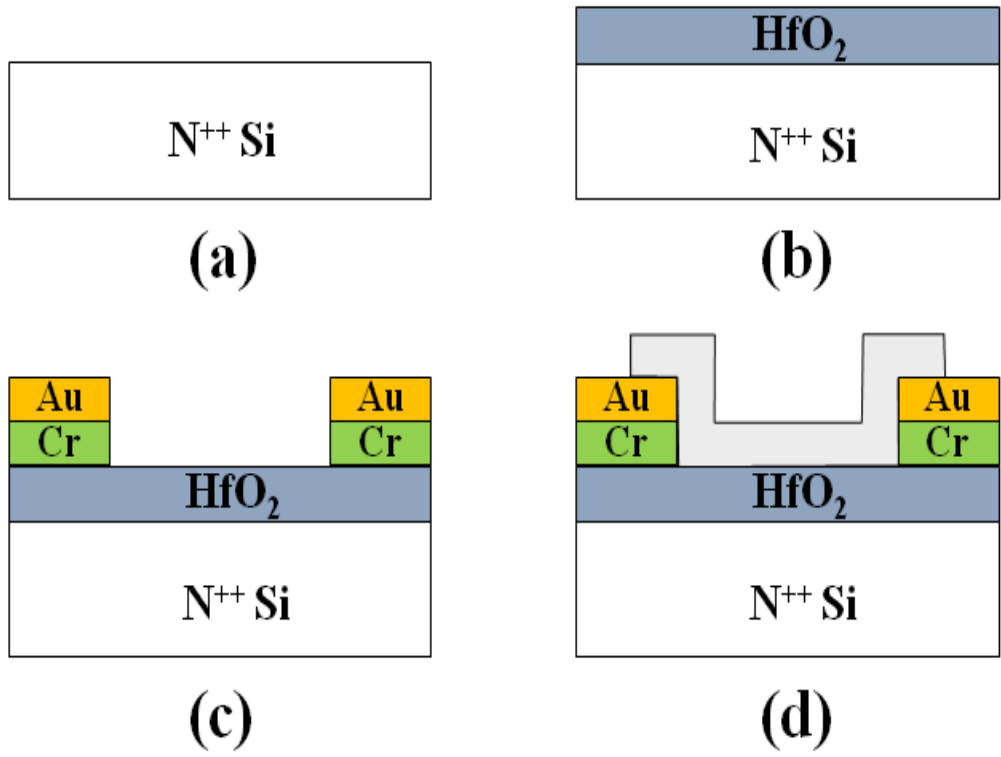


Fig.1. Cross-sectional views of key fabrication steps. Heavily doped N<sup>++</sup> Si substrate is used a bottom-gate.

## 2.2 Surface characterization

Raman spectrum and optical transmittance of the graphene grown by using the ICP-CVD are shown in [8], [9]. Fig2. Shows single layer graphene was confirmed by Raman spectroscopy with a single Lorentzian fit of a 2D peak at  $2700\text{ cm}^{-1}$ . The 2D name originally comes from the fact that 2D band is located at Raman shift of  $2700\text{ cm}^{-1}$  which is twice the value of the Raman shift of D band ( $1350\text{ cm}^{-1}$ ) [8][9]. The  $I_{2D}/I_G$  (intensity of 2D peak / intensity of G peak) ratio for graphene exceed 4, conforming single layer graphene film [10]. In addition, we observed relatively weak D peak intensity ( $I_D/I_G$ ), which indicates the minimum level of structural defects in our samples. Fig3. Shows optical transmittance data also could be known method to evaluate layer number with 2.3% reduction of one layer at 550 nm and our sample shows exactly 97.7% transmittance [11]. Those clearly indicate that the transferred graphene is a single layer and has high-purity carbon in the graphene films. The channel length and width of the graphene FETs are  $8\text{ }\mu\text{m}$  and  $2\text{ }\mu\text{m}$ , respectively.

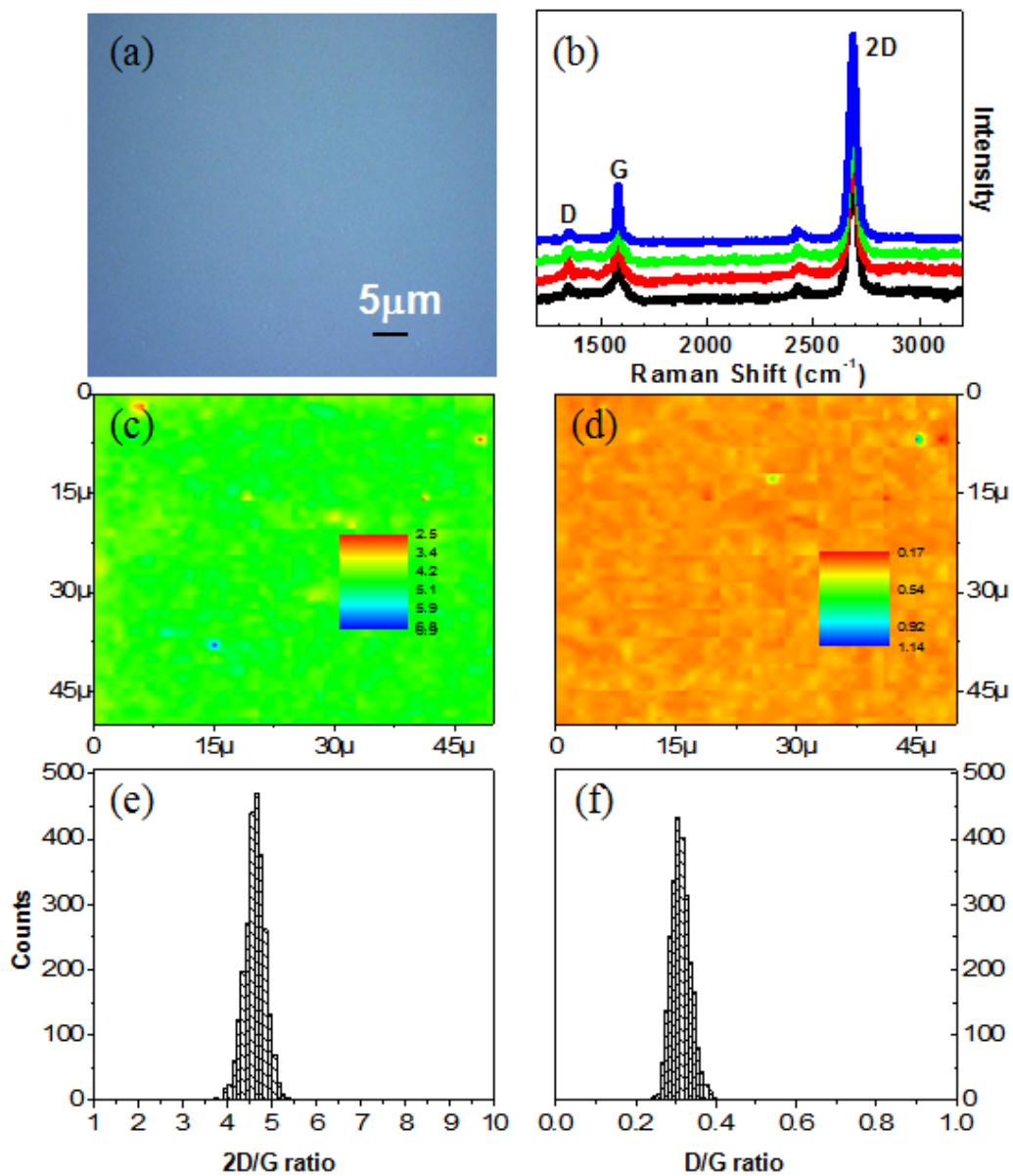


Fig. 2 (a) The optical image of transferred graphene onto SiO<sub>2</sub>. Raman mapping and distribution of 50 μm x 50 μm area 2D/G ratio (c, e) and D/G ratio (d, f)[9]

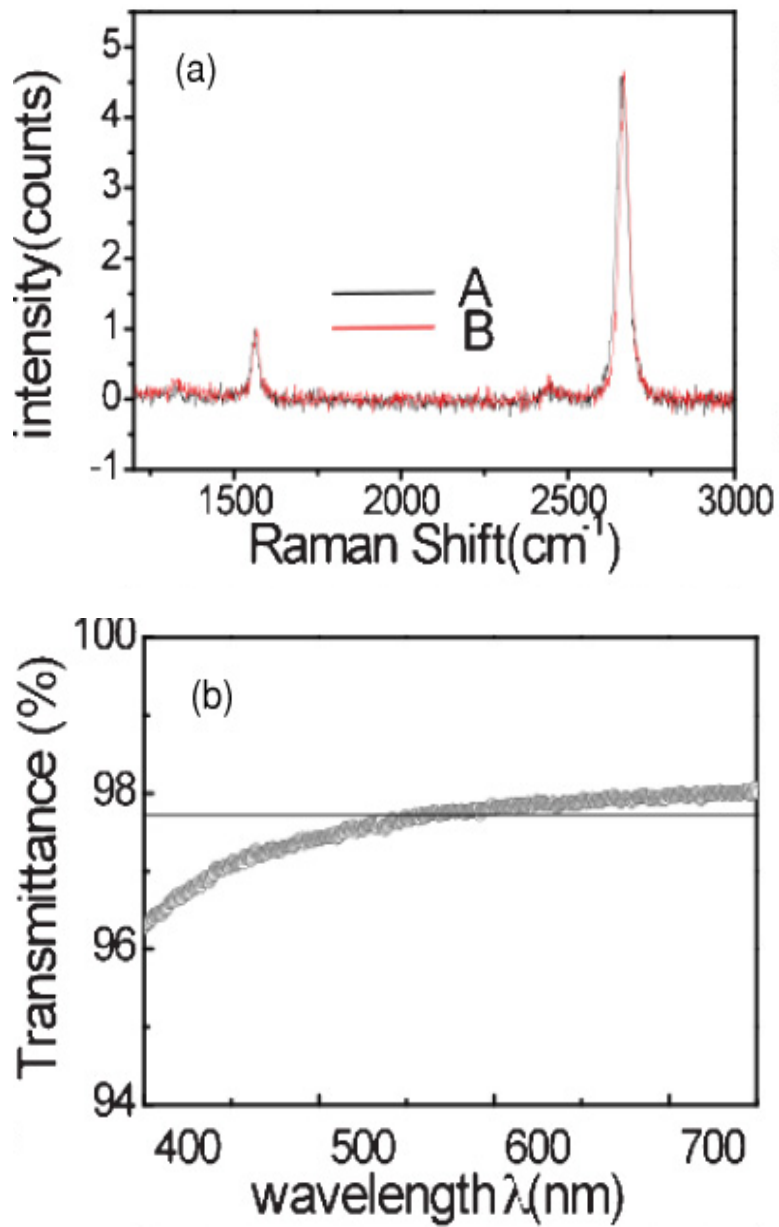


Fig. 3. (Color online) (a) Raman spectroscopy on a device. Inset: Optical microscope image of a device. (b) Light transmittance through CVD grown single layer graphene/glass [8].

## **3. Analysis of Gas sensing Characteristic on Bottom Gate Graphene FET**

### **3.1 Gas sensing on bottom gate graphene FET**

To measure gas sensitivity, the wafer including graphene FETs was placed inside a sealed chamber in which gas supply line and pump line are connected. Electrical measurement was carried out using an Agilent 4155C.  $\text{NO}_2$ ,  $\text{NH}_3$  prepared by intermixing calibrated commercial gases with nitrogen ( $\text{N}_2$ ) are used and humid gas was obtained by flowing nitrogen through a bubbler. Different relative humidity levels and gases concentration were controlled with a mass flow controller (MFC). In this experiment,  $\text{NO}_2$ ,  $\text{NH}_3$ ,  $\text{H}_2\text{S}$ ,  $\text{SO}_2$ ,  $\text{CH}_4$ , and  $\text{C}_3\text{H}_8$  prepared by intermixing calibrated commercial gases with  $\text{N}_2$  are used. We measured  $I_D$ - $V_{GS}$  (the conductivity vs gate bias) characteristic at room temperature under one atmospheric pressure after exposing the device to a specific gas for 1 hour (saturation state) in a chamber.

We measured  $I_D$ - $V_{GS}$  transfer curve at room temperature under one

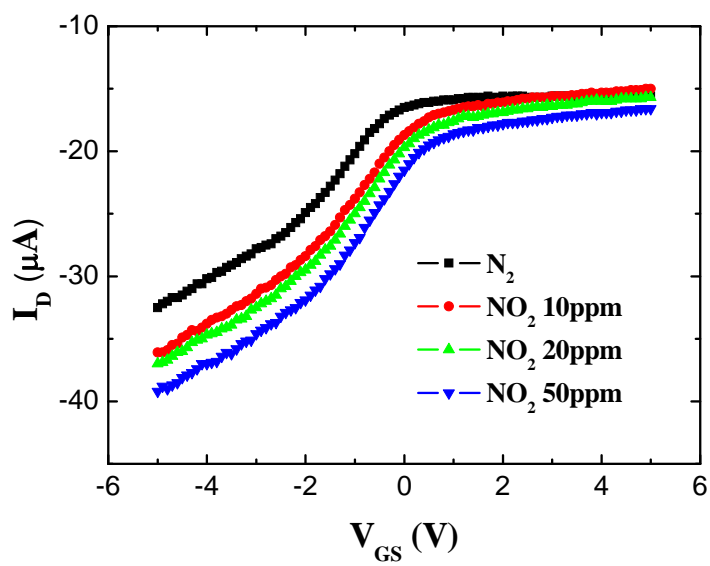
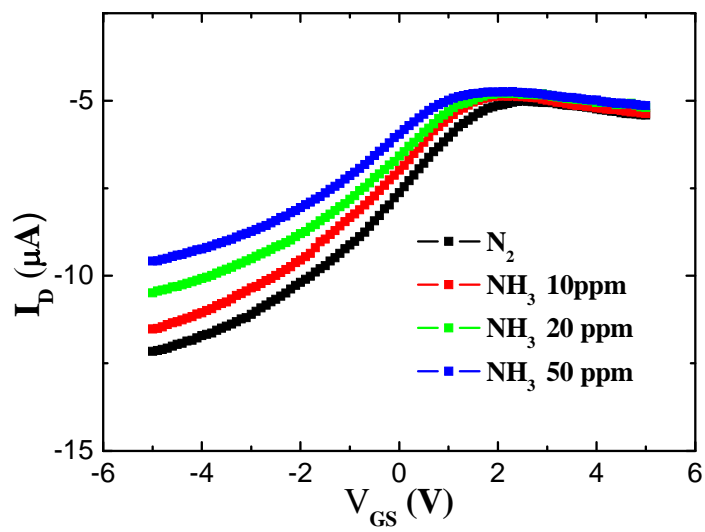
atmospheric pressure after exposing the graphene devices to air. The transfer curve exhibits asymmetric behavior and p-type MOS characteristic. Generally, CVD grown graphene shows the asymmetric behavior in hole and electron conduction along with the Dirac point shift. Graphene in this study was exposed in the air and hole doping due to the oxygen and water molecule could be considered according to the temperature dependence[16]. The origin of this behavior might be caused by a combination of the neutrality point misalignment at the electrode/channel interface and the nonconstant DOS (Density of State) of the graphene by chemical doping (hole and electron)[17]. In engineering point of view, sensing area of all gas sensors must be exposed practically in the air to detect a target gas. So we measure our graphene FETs not in vacuum (low pressure) but in air (atmospheric pressure). Gate bias ( $V_{GS}$ ) scans from -5 V to 5 V at  $V_{DS} = -10$  mV.

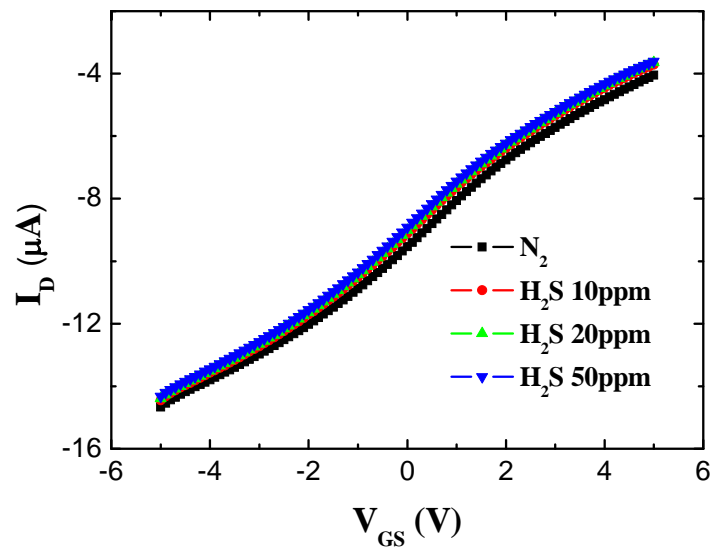
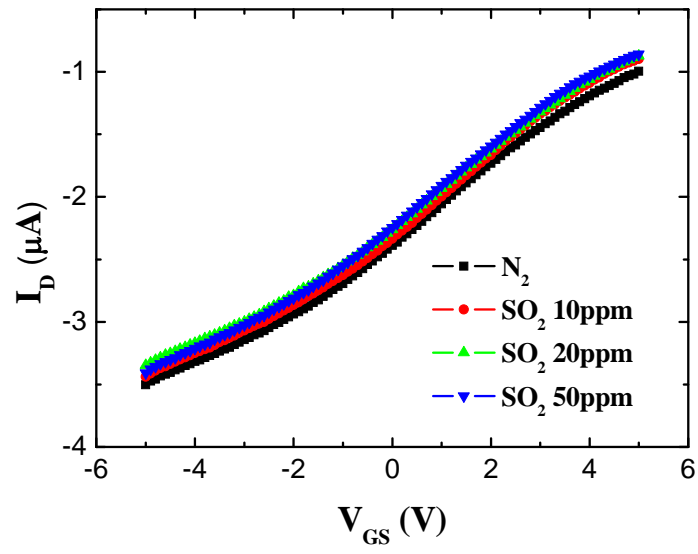
Six devices are used to investigate sensing property for 6 different gases mentioned above. Fig.4 shows  $I_D$ - $V_{GS}$  curves of the graphene FETs as a parameter of gas concentration (ppm) at a fixed  $V_{DS}$  of -10 mV. The channel

length and width of the graphene FETs are 8  $\mu\text{m}$  and 2  $\mu\text{m}$ , respectively. We can observe clearly the sensitivity with a specific gas and summarize the results in Fig. 5. Fig.5 (a) and (b) show the gas concentration dependency of conductivity change (sensitivity) measured at a  $V_{\text{GS}}$  of -3 V for 6 different gases. Here the conductivity change is defined as

$$\left[ (I_D - I_{D0}) / I_{D0} \right] \times 100\% \quad (1)$$

Where the drain current change ( $I_D - I_{D0}$ ) with respect to that in  $\text{N}_2$  (reference drain current:  $I_{D0}$ ) at  $V_{\text{GS}} = -3$  V.  $I_D$  is the drain current with a concentration of a gas. With increasing gas concentration, the conductivity of graphene exposed to  $\text{NO}_2$  increases, whereas the conductivity for other gases decreases.  $\text{NO}_2$  and  $\text{NH}_3$  absorbed on graphene act as acceptor and donor, respectively [1]. Both gases show relatively large sensitivity. In the case of  $\text{SO}_2$  and  $\text{H}_2\text{S}$ , there is little change in conductivity. Since  $\text{CH}_4$  and  $\text{C}_3\text{H}_8$  gases show even smaller sensitivity than that of  $\text{SO}_2$  and  $\text{H}_2\text{S}$  gases, the concentration is increased up to  $10^4$  ppm. However, both  $\text{CH}_4$  and  $\text{C}_3\text{H}_8$  gases show the sensitivity less than  $\sim 8\%$  at  $10^4$  ppm.





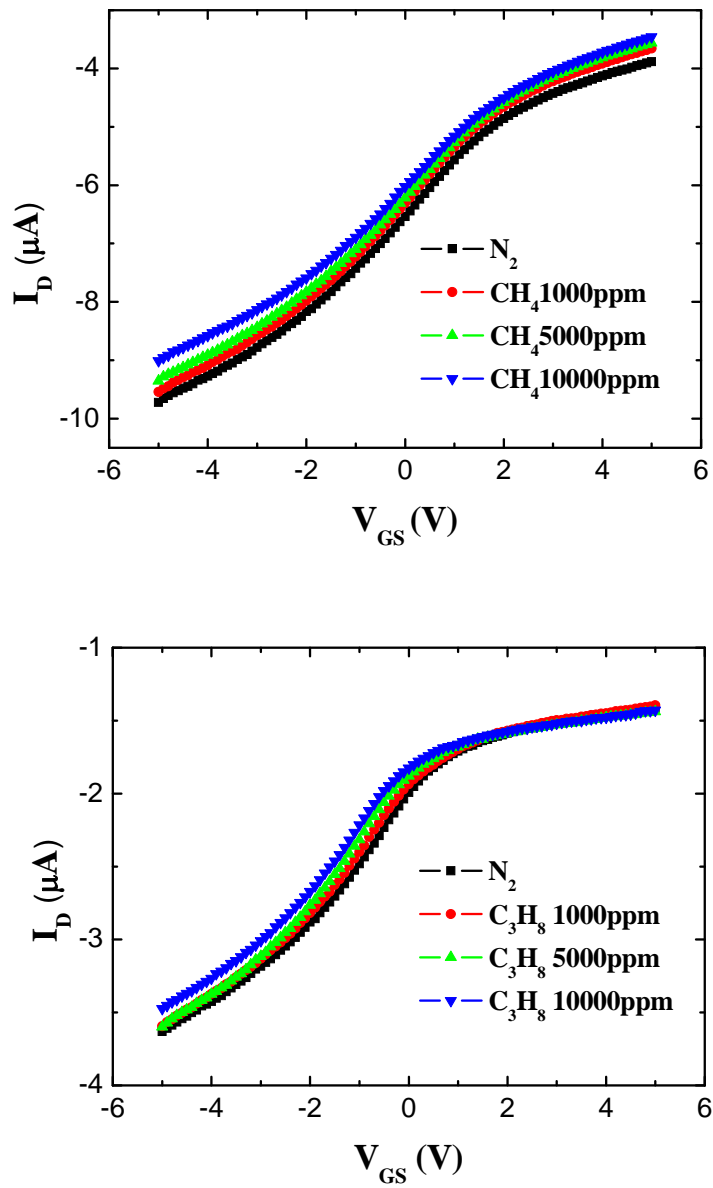


Fig.4. The change in transfer characteristic for graphene exposed to different gases concentrations (a)  $\text{NH}_3$ , (b)  $\text{NO}_2$ , (c)  $\text{H}_2\text{S}$ , (d)  $\text{SO}_2$ , (e)  $\text{CH}_4$ , (f)  $\text{C}_3\text{H}_8$  ( $V_{DS} = -10 \text{ mV}$  and  $V_{GS} = -5 \sim 5 \text{ V}$ )

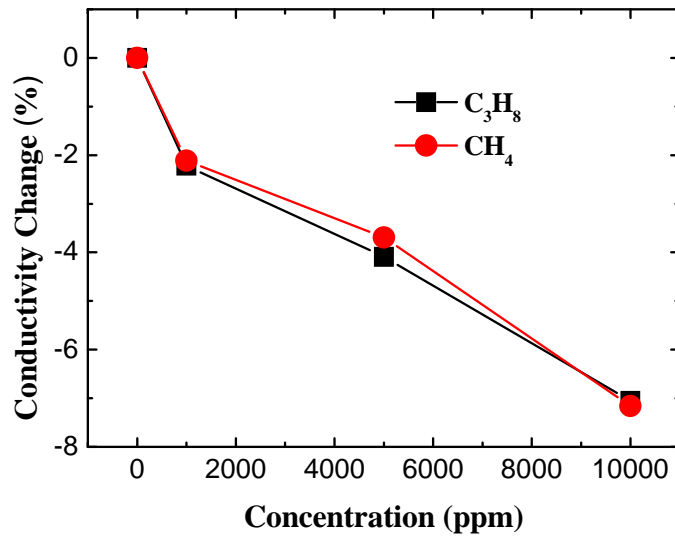
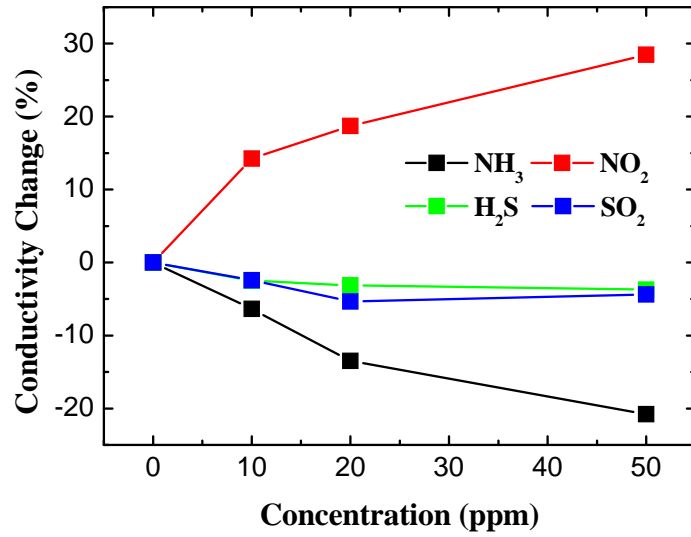


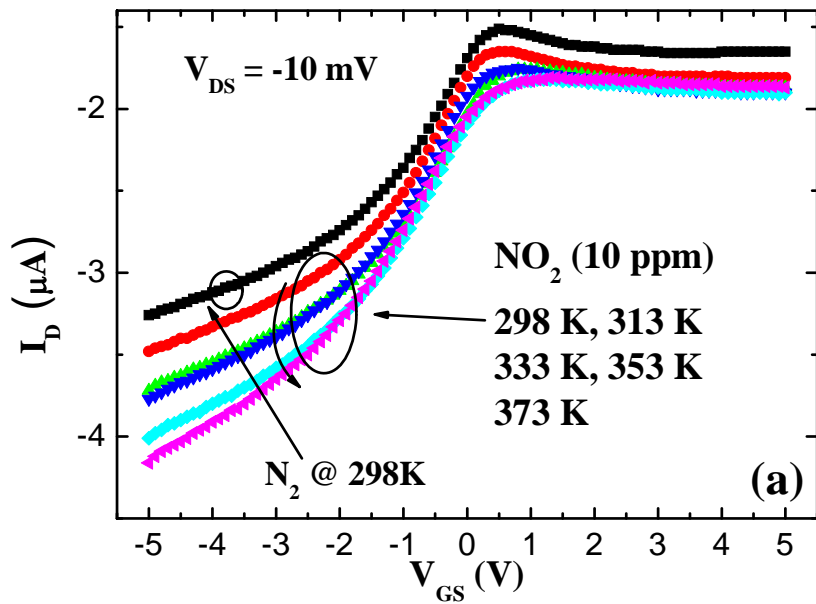
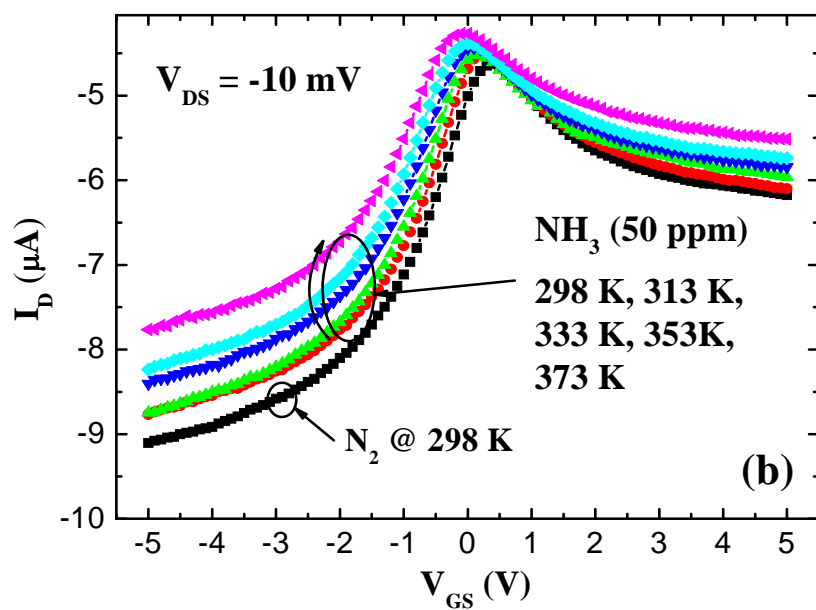
Fig.5. The change in conductivity for graphene exposed to different gases concentrations (a) NH<sub>3</sub>, NO<sub>2</sub>, H<sub>2</sub>S, SO<sub>2</sub> (b) CH<sub>4</sub>, C<sub>3</sub>H<sub>8</sub>

## 3.2 Effect of Temperature and Humidity on NO<sub>2</sub> and NH<sub>3</sub> Gas Sensitivity of Bottom-Gate Graphene FETs

Fig. 6 shows the  $T$  dependency of conductivity change for two different target gases (NO<sub>2</sub>, and NH<sub>3</sub>). In each measurement, we used fresh graphene FET to rule out any problem which can be generated during repeated measurement. As a control  $I_D$ - $V_{GS}$  curve, we first measure  $I_D$ - $V_{GS}$  curve in  $N_2$  ambient for each sample, and then measure conductivity change with a target gas. As mentioned above, the conductivity change is defined as (1) where  $I_D$  is a drain current at  $V_{GS}=-3$  V with different temperature ( $T$ ) or relative humidity (RH), and  $I_{D0}$  is the  $I_D$  (@ $V_{GS} =-3$  V) under the first condition of a target gas (for example, NO<sub>2</sub> at 298K or 0% of RH). Graphene gas sensor in this work shows about 20 - 30 % conductivity change for both NO<sub>2</sub> and NH<sub>3</sub> as the concentration changes from 0 to 50 ppm. The gases used in this experiment are N<sub>2</sub> (pure), NO<sub>2</sub> (10 ppm) and NH<sub>3</sub> (50ppm), respectively. In this experiment, we found the conductivity

change with  $T$  (298 K  $\sim$  373 K). The drain current ( $I_D$ ) of graphene exposed to  $\text{NO}_2$  increases, whereas the drain current for  $\text{NH}_3$  decreases as shown in Fig. 6 (a) and (b), respectively, because  $\text{NO}_2$  and  $\text{NH}_3$  absorbed on graphene act as acceptor and donor, respectively [1]. As the  $T$  increases, graphene FETs in this work show increasing  $I_D$  for  $\text{NO}_2$  gas (a) and decreasing  $I_D$  for  $\text{NH}_3$  gas (b) in magnitude. Conductivity change with  $T$  obtained by using (1) is shown in Fig. 6 (c). Solid square and circle symbols represent the changes with  $T$  for  $\text{NO}_2$  and  $\text{NH}_3$ , respectively. The conductivity change of graphene FETs in  $\text{N}_2$  ambient decreased with a rate of  $\sim 0.1\ \%/^\circ\text{C}$  because the graphene has a metallic property. By subtracting the conductivity change with  $T$  in  $\text{N}_2$  ambient, we could extract the conductivity changes for  $\text{NO}_2$  and  $\text{NH}_3$  gases as indicated by triangle and inverse triangle symbols. In Fig. 6 (c), as  $T$  increases,  $I_D$  for  $\text{NO}_2$  gas increases although the metallic property decreases the  $I_D$  while the  $I_D$  decreases more significantly in  $\text{NH}_3$  ambient than in  $\text{N}_2$  ambient with increasing  $T$ . Conductivity change seems to be related to the amount of hole ( $\text{NO}_2$ ) and electron ( $\text{NH}_3$ ) charge transfer and to the nature of the surface interaction of the gas and

graphene by the increased  $T$  [14].



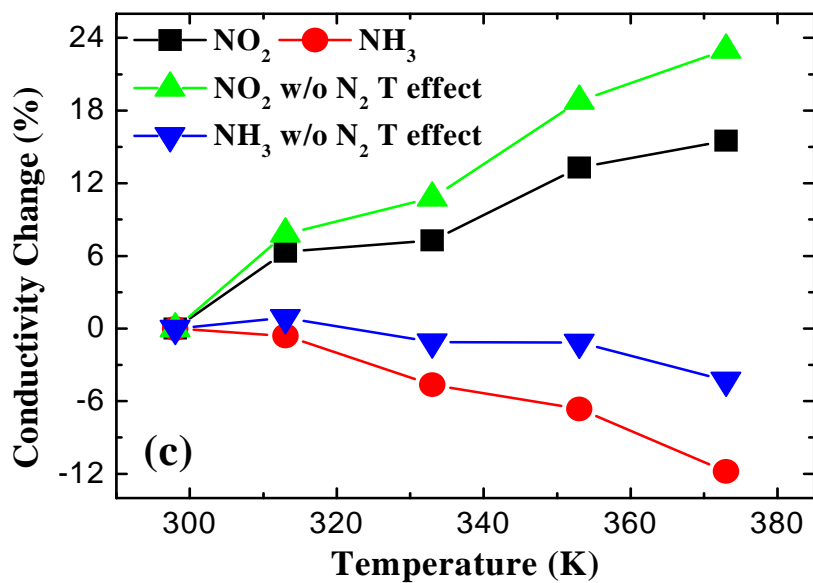
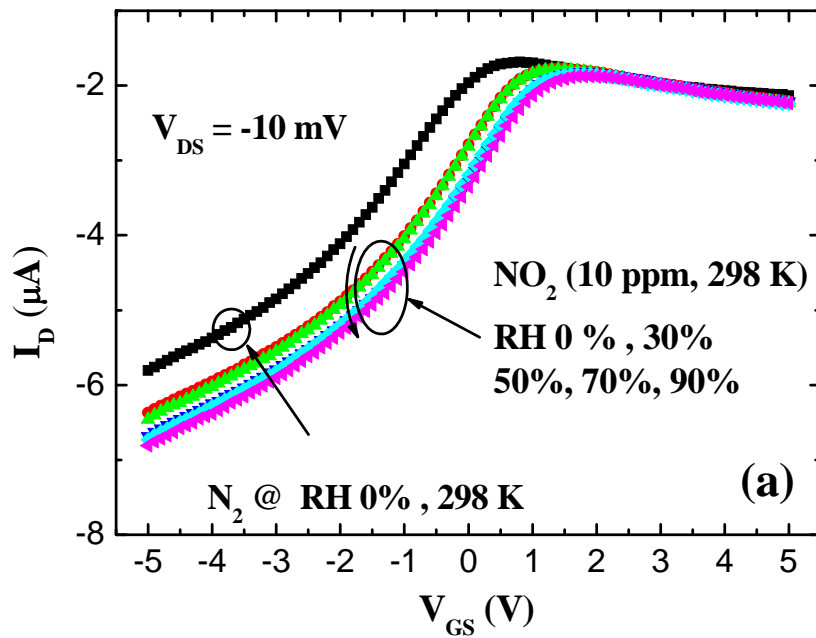


Fig.6. I-V characteristics for graphene FETs exposed to 10 ppm NO<sub>2</sub> (a) and 50 ppm NH<sub>3</sub> (b) as a parameter of temperature. Conductivity change versus temperature is shown for both gases (c). A target gas without N<sub>2</sub> T effect means that the conductivity change with T in N<sub>2</sub> ambient is excluded.

Fig. 7 shows the humidity dependency of conductivity change for two target gases ( $\text{NO}_2$  and  $\text{NH}_3$ ). The RH was changed from 0 % (mixed gas) to 90 % at room temperature. As the RH increases, graphene FETs in this work show increasing  $I_D$  for  $\text{NO}_2$  gas (a) and decreasing  $I_D$  for  $\text{NH}_3$  gas (b). In Fig. 7 (c), we can observe the conductivity changes for  $\text{NO}_2$  and  $\text{NH}_3$  gases with RH as represented by solid square and circle symbols, respectively. As the RH increases, graphene FETs in  $\text{N}_2$  ambient increased with a rate of  $\sim 0.58\ \%/%$  because the humidity absorbed on graphene acts as acceptor. Fig. 7 (c) also shows the conductivity changes for  $\text{NO}_2$  (triangle symbols) and  $\text{NH}_3$  (inverse triangle symbols) gases by excluding the change with RH in  $\text{N}_2$  ambient. Since the humidity and  $\text{NO}_2$  act as acceptor, their effects are added. In case of  $\text{NH}_3$ , the conductivity change increases with the increase of RH. Humidity and  $\text{NH}_3$  have the opposite effect on the conductivity of graphene: humidity and  $\text{NH}_3$  act as acceptor and donor, respectively. Therefore we can expect that the RH effect cancels out the effect of  $\text{NH}_3$  and the  $I_D$  change is expected to be quite small. However,  $\text{NH}_3$  and humidity form ammonium hydroxide ( $\text{NH}_4\text{OH}$ ) by the

reaction in the chamber. Since the  $\text{NH}_4\text{OH}$  absorbed on graphene acts as donor [15], the conductivity change of graphene exposed to ammonia increases negatively with increasing RH.



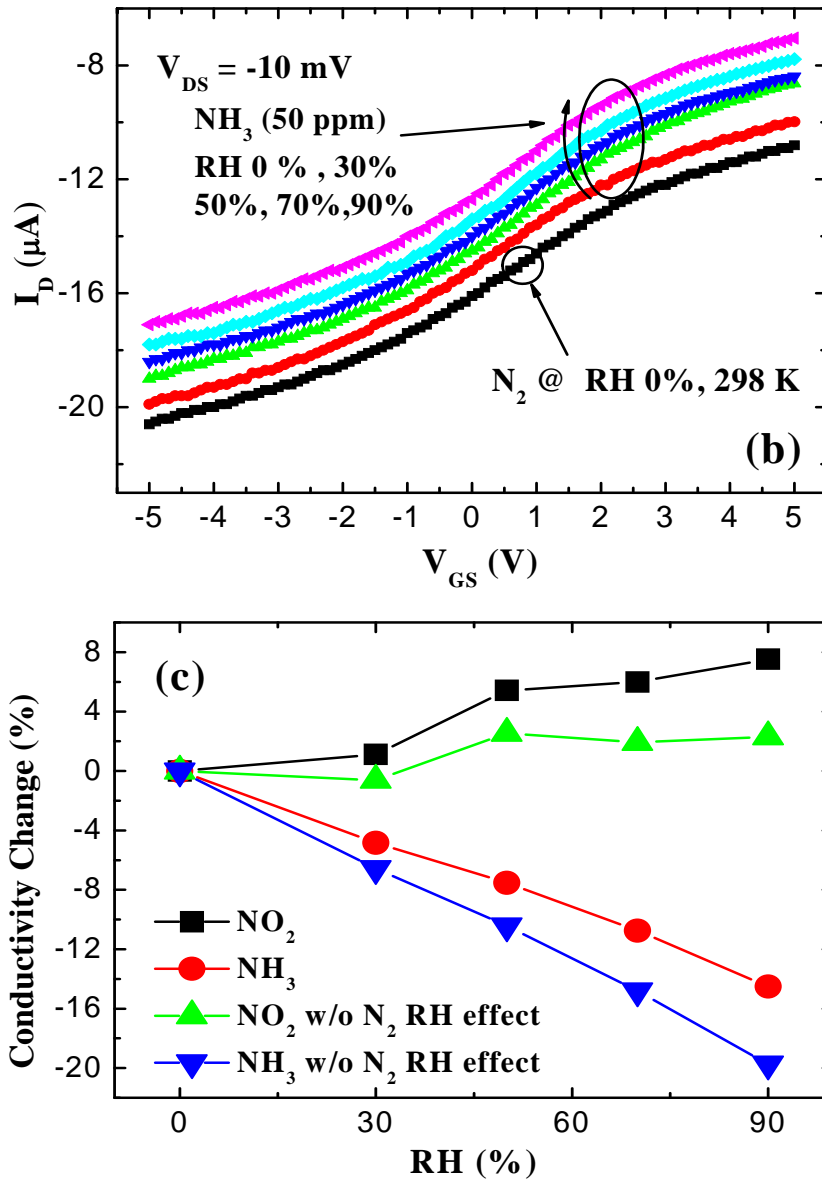


Fig.7. I-V characteristics for graphene FETs exposed to  $10\text{ ppm}$   $\text{NO}_2$  (a) and  $50\text{ ppm}$   $\text{NH}_3$  (b) as a parameter of relative humidity (RH) at  $298\text{ K}$ . Conductivity change versus RH is shown for both gases (c). A target gas without  $\text{N}_2$  RH effect means that the conductivity change with RH in  $\text{N}_2$  ambient is excluded

## 5. Conclusion

In this master's thesis, we have investigated gas sensing characteristic of Bottom gate FETs with single atomic graphene layer grown on 6-inch wafer using low temperature ICP-CVD method at 650 °C. We quantitatively analyzed sensitivity of various gases ( $\text{H}_2\text{S}$ ,  $\text{NH}_3$ ,  $\text{NO}_2$ ,  $\text{SO}_2$ ,  $\text{CH}_4$ ,  $\text{C}_3\text{H}_8$ ), temperature and humidity effects for at  $\text{NO}_2$  and  $\text{NH}_3$  gases. The devices showed relatively large conductivity change (20%~30% at 50 ppm) for both  $\text{NO}_2$  (positive change) and  $\text{NH}_3$  (negative change) gases. With increasing temperature, the drain current increases for  $\text{NO}_2$  but decreases for  $\text{NH}_3$  by the increased surface interaction due to increased temperature.  $\text{NO}_2$  and humidity acted as acceptor on the graphene and their effects were added. It was found that  $\text{NH}_3$  reacts with humidity to form  $\text{NH}_4\text{OH}$  which acts as donor on the graphene and consequently the drain current decreases. The bottom-gate graphene FETs fabricated by using ICP-CVD could be low cost and high sensitive gas sensors.

## References

- [1] F. Schedin, A. K. Geim, S. V. Morozov, E. W. Hill, P. Blake, M. I. Katsnelson, and K. S. Novoselov, “Detection of individual gas molecules adsorbed on graphene”, *Nature Materials*, vol. 6, pp. 652–655, Jul. 2007.
- [2] Yuanbo Zhang, Yan-Wen Tan, Horst L. Stormer and Philip Kim, “Experimental observation of the quantum Hall effect and Berry's phase in graphene”, *Nature*, vol. 438, pp. 201-204, Nov. 2005.
- [3] X. Li, W. Cai, J. An, S. Kim, J. Nah, D. Yang, R. Piner, A. Velamakanni, I. Jung, E. Tutuc, S. K. Banerjee, L. Colombo, and R. S. Ruoff, “Large-Area Synthesis of High-Quality and Uniform Graphene Films on Copper Foils”, *Science*, vol. 324, pp. 1312-1314, May 2009.
- [4] United State Environmental Protection Agency (EPA). [Online]. Available : <http://www.epa.gov>

- [5] Suk ju Hwang, Joon Hyong Cho, Juw han Lim, Whan Kyun Kim, Hyun jin Shin, J.Y. Choi, J.H. Choi, Sang Yoon Lee, J.M. Kim, Jae Hun Kim, Seok Lee, Chan Jun Seong, “Graphene based NO<sub>2</sub> gas sensor”, *Nanotechnology Materials and Devices Conference (NMDC)*, Oct. 2010, pp. 12-15
- [6] R. Pearce, T. Iakimov, M. Andersson, L. Hultman, A. Lloyd Spetz, R. Yakimova, “Epitaxially grown graphene based gas sensors for ultrasensitive NO<sub>2</sub> detection”, *Sensors and Actuators B*, vol. 155 no.2, pp. 451-455, Jul. 2011.
- [7] Madhav Gautam, Ahalapitiya H. Jayatissa, “Gas sensing properties of graphene synthesized by chemical vapor deposition”, *Materials Science and Engineering C*, May 2011. (Available online)
- [8] J. Heo, H. J. Chung, Sung-Hoon Lee, H. Yang, D. H. Seo, J. K. Shin, U-In Chung, S. Seo, E. H. Hwang, and S. Das Sarma, “Nonmonotonic temperature dependent transport in graphene grown by chemical vapor deposition”, *Phys. Rev. B*, vol. 84, no. 3 pp. 35421-35427, Jul. 2011

- [9] Jaeho Lee, Hyun-Jong Chung, Jaehong Lee, Hyungcheol Shin, Jinseong Heo, Heejun Yang, Sung-Hoon Lee, Sunae Seo, Jaikwang Shin, U-in Chung, Inkyeong Yoo and Kinam Kim. “RF performance of pre-patterned locally-embedded-back-gate graphene device”, in *IEDM Tech. Dig.*, 2010, pp. 568–571.
- [10] A. C. Ferrari, J. C. Meyer, V. Scardaci, C. Casiraghi, M. Lazzeri, F. Mauri, S. Piscanec, D. Jiang, K. S. Novoselov, S. Roth, and A. K. Geim, “Raman spectrum of graphene and graphene layers”, *Phys. Rev. Lett.* vol, 97, no.18, pp. 187401-187404, Oct. 2006.
- [11] R. R. Nair, P. Blake, A. N. Grigorenko, K. S. Novoselov, T. J. Booth, T. Stauber, N. M. R. Peres, and A. K. Geim, “Fine Structure Constant Defines Visual Transparency of Graphene”, *Science*, vol. 320, no. 5881 , p.1308, Apr. 2008.
- [12] P.L. Levesque, S.S. Sabri, C.M. Aguirre, J. Guillemette, M. Siaj, P. Desjardins, T. Szkopek, and R. Martel, “Probing Charge Transfer at Surfaces

- Using Graphene Transistors”, *Nano Lett.* vol. 11, no.1, pp.132-137, Dec. 2011
- [13] A.N. Sidorov, A. Sherehiy, R. Jayasinghe, R. Stallard, D.K. Benjamin, Q.K. Yu, Z.H. Liu, W. Wu, H.L. Cao, Y.P. Chen, Z. Jiang, and G.U. Sumanasekera, "Thermoelectric power of graphene as surface charge doping indicator", *Appl. Phys. Lett.* vol. 99, no.1 pp. 013115-013117, July. 2011.
- [14] Y. -T. Jang, S. -I. Moon, J. -H. Ahn, Y. -H. Lee, and B. -K. Ju, "A simple fabricating chemical sensor using laterally grown multi-walled carbon nanotubes", *Sensors and Actuators B*, vol. 99, no. 1, pp. 118-122, Apr. 2004
- [15] H. Pinto, R. Jones, J. P. Goss, and P. R. Briddon "Mechanisms of doping graphene", *Phys. Status Solidi A*, vol. 207, no. 9, pp. 2131–2136, Aug. 2010.
- [16] P.L. Levesque, S.S. Sabri, C.M. Aguirre, J. Guillemette, M. Siaj, P. Desjardins, T. Szkopek, and R. Martel, "Probing Charge Transfer at Surfaces Using Graphene Transistors”, *Nano Lett.* vol. 11, no.1, pp.132-137, Dec. 2011.
- [17] Damon B. Farmer, Rokhsana Golizadeh-Mojarad, Vasili Perebeinos, Yu-

Ming Lin, George S. Tulevski, James C. Tsang, and Phaedon Avouris,  
“Chemical Doping and Electron-Hole Conduction Asymmetry in Graphene  
Devices” *Nano Lett.* vol 9, no.1 pp.388-392 Dec. 2009.

## 초 록

최근 높은 민감도 및 선택성을 가지고 제조 비용이 낮은 가스센서의 수요가 증가하고 있다. 이러한 특성을 가진 가스센서를 구현하기 위해 현재 그래핀(graphene)의 가스 반응에 대한 연구를 진행 중에 있다. (그래핀은 이산화질소( $\text{NO}_2$ )와 암모니아( $\text{NH}_3$ )에 큰 민감도 (Sensitivity)를 가진다.) 현재 그래핀 제작 방법으로는 스킵치테이프를 이용한 exfoliation 방법, 실리콘카바이드(SiC)기판을 높은 온도로 가열하여 그래핀을 제조하는 방법 및 최근 높은 진공도에서 탄화수소를 촉매 금속에 흐리는 화학적 기상 증착 방법을 이용한 방식이 개발되었다. 최근에는 낮은 온도에서 고품질의 그래핀 제조 방법으로 inductively coupled plasma chemical vapor deposition (ICP-CVD)를 이용한 연구가 진행 되고 있다. ICP-CVD 방법은 약 650도에서 공정이 가능하다. 하지만 ICP-CVD 방법으로 제조된 그래핀의 가스 반응 특성 및 가스 반응시 온도 및 습도가 민감도에 미치는 영향에 대해서는 자세한 연구

결과가 아직까지 보고되지 않았다.

본 논문에서는 ICP-CVD 방법으로 제조된 Bottom게이트 구조의 그래핀 FET를 이용하여 가스 반응의 민감도 및 가스 반응시 온도 및 습도의 영향에 대한 연구를 진행하였다. 실험 결과 그래핀은 암모니아(농도가 50ppm 일때 대략 20 %정도) 및 이산화질소(농도가 50ppm 일때 대략 30 %정도)에서 상대적으로 높은 가스 민감도가 나타났다. 황화수소( $H_2S$ ), 이산화황( $SO_2$ ), 메탄( $CH_4$ ) 프로판( $C_3H_8$ )에서는 반응이 크게 나타나지 않았다. 심지어 메탄 및 프로판은 각각의 가스 농도가 10000ppm 에서도 민감도가 10 %가 미만으로 나타났다. 그래핀이 일정 이산화질소 및 암모니아 농도에서 각각의 가스와 반응할 때 온도 및 수분이 증가하면 민감도가 증가하는 결과를 나타내었다. 이산화 질소에서는 온도 및 수분이 증가하면 그래핀의 드레인 전류를 증가 시켰다. 하지만 암모니아에서는 반응 온도 및 수분이 증가하면 이산화 질소와는 반대 경향이 나타났다. 이런 가스반응 특성들은 신뢰성 있는 그래핀 가스 센서 설계에 사용될 수 있을 것으로 예상된다.

주요어: 그래핀, 가스센서, 민감도 ,Bottom 게이트, 온도, 습도

학번: 2010-232354